

## Original article

Characterization of exclusive rib lesions detected by [<sup>68</sup>Ga]Ga-PSMA-11 PET/CTMarine Stoffels<sup>a</sup>, François Cousin<sup>a</sup>, Maréva Lamande<sup>b</sup>, Chloé Denis<sup>c</sup>, David Waltregny<sup>d</sup>, Roland Hustinx<sup>a,e</sup>, Briec Sautois<sup>c,\*</sup> and Nadia Withofs<sup>a,e,\*</sup>

**Objective** The objective of this study was to characterize exclusive costal lesions detected by <sup>68</sup>Gallium-labelled prostate-specific membrane antigen ([<sup>68</sup>Ga]Ga-PSMA-11) PET/computed tomography (CT) at initial staging or biochemical recurrence (BCR) in prostate cancer (PCa) patients, and to identify clinical and/or PET/CT criteria associated with benign and malignant lesions.

**Methods** We retrospectively identified 54 patients with PCa who underwent [<sup>68</sup>Ga]Ga-PSMA-11 PET/CT for initial staging (*N* = 39) or BCR (*N* = 15) and whose reports described rib lesions, at the exclusion of any other lesions, whether doubtful, suspicious, or established. Posttherapy prostate-specific antigen (PSA) levels were used to determine whether those lesions were benign or malignant. Each patient's prostate-specific membrane antigen PET/CT report was classified as true positive, true negative, false positive, or false negative based on the posttherapy PSA level. We then assessed whether any clinical and/or PET/CT criteria could help differentiate benign from malignant lesions, and if any criteria were misleading.

**Results** Among the 54 patients, 46 (85.2%) had 64 benign costal lesions, and eight (14.8%) had 10 malignant lesions. PET/CT reports indicated rib lesions as benign/equivocal in 38/54 (55.6%) patients and malignant in

16/54 (29.6%). Benign features on CT were the only parameter significantly associated with the final diagnosis. Factors such as patient age, maximum standardized uptake value of lesions, lesion dispersion, and malignant features described on CT were found to be misleading when deciding the malignant or benign status.

**Conclusion** Most exclusive costal lesions detected by [<sup>68</sup>Ga]Ga-PSMA-11 PET/CT are benign. Apart from specific benign CT features, no clinical or PET/CT criteria reliably differentiate benign from malignant costal lesions. *Nucl Med Commun* XXX: XXXX-XXXX Copyright © 2024 The Author(s). Published by Wolters Kluwer Health, Inc.

Nuclear Medicine Communications XXX, XXX:XXXX-XXXX

**Keywords:** bone, costal, imaging, PET, pitfall, prostate, prostate-specific membrane antigen, rib, unspecific

<sup>a</sup>Division of Nuclear Medicine and Oncological Imaging, Department of Medical Physics, University Hospital of Liege, Departments of <sup>b</sup>Radiation Therapy, <sup>c</sup>Medical Oncology, <sup>d</sup>Urology, University Hospital of Liège, CHU Sart Tilman and <sup>e</sup>GIGA-CRC in Vivo Imaging, University of Liege, Liege, Belgium

Correspondence to Marine Stoffels, MD, Division of Nuclear Medicine and Oncological Imaging, Department of Medical Physics, University Hospital of Liege, Quartier Hôpital, Avenue de l'Hôpital 1, 4000 Liege 1, Belgium  
Tel: +32 43215589; e-mail: marine.stoffels@chuliege.be

\*Briec Sautois and Nadia Withofs contributed equally to the writing of this article.

Received 24 July 2024 Accepted 2 October 2024.

## Introduction

Prostate cancer (PCa) is the most common and frequently diagnosed cancer in men in Europe, after skin cancers [1]. In 2022, an estimated 1.5 million cases were diagnosed, with 397 000 deaths globally [2]. It is the fifth leading cause of cancer mortality worldwide and the third in Europe [3]. Prostate-specific membrane antigen (PSMA) PET combined with computed tomography (CT) has significantly advanced the field of PCa imaging, offering higher sensitivity and specificity than conventional imaging, bone scintigraphy, and CT, in staging high-risk PCa

patients and for earlier detection of the site of recurrence at lower prostate-specific antigen (PSA) levels [4–11].

Bones are the most common metastatic site of PCa, especially the ribs, pelvis, and spine, where hematopoietic bone marrow is abundant. Bone metastases can present as osteolytic, osteosclerotic, or mixed lesions, depending on the interplay between tumor cells and the bone microenvironment. Osteosclerotic lesions are the most common in PCa [12]. PSMA-targeted radioligands may also lead to false positives (FPs) due to PSMA overexpression in angiogenesis and/or by cancer cells of other cancer types [13–17]. Benign bone conditions such as Paget's disease, fibrous dysplasia, vertebral hemangiomas, degenerative changes, and fractures can exhibit significant PSMA uptake on PET/CT scans, potentially leading to FP results that could prompt inappropriate patient management. Unspecific bone uptakes (UBUs) of PSMA-targeted radioligands have been reported in PCa patients with varying frequencies: from 0 to 23.9%

Supplemental Digital Content is available for this article. Direct URL citations appear in the printed text and are provided in the HTML and PDF versions of this article on the journal's website, [www.nuclearmedicinecomm.com](http://www.nuclearmedicinecomm.com).

This is an open-access article distributed under the terms of the Creative Commons Attribution-Non Commercial-No Derivatives License 4.0 (CCBY-NC-ND), where it is permissible to download and share the work provided it is properly cited. The work cannot be changed in any way or used commercially without permission from the journal.

for  $^{68}\text{Ga}$ -labelled prostate-specific membrane antigen ( $^{68}\text{Ga}$ )Ga-PSMA-11), from 11.6 to 71.7% for  $^{18}\text{F}$  PSMA-1007, and in 19.8% for  $^{18}\text{F}$  DCFPyl and 24% for  $^{18}\text{F}$  rhPSMA-7 in single studies [15,18–28]. These UBUs are predominantly observed in the ribs, spine, and pelvis [18,19,28,29]. Interpreting bone lesions may be particularly challenging with  $^{18}\text{F}$  PSMA-1007 compared with  $^{68}\text{Ga}$ )Ga-PSMA-11 due to higher incidence of UBUs, potentially leading to over-staging and inappropriate treatment decisions if misinterpreted [18,29]. Incorporating CT images with PET and reviewing previous scans, or employing additional MRI, facilitates accurate diagnosis [13,14].

As highlighted in the recent systematic review by Rizzo *et al.* [28], the ribs are identified as the primary site of UBUs across all PSMA-targeted radiopharmaceuticals. Furthermore, unspecific rib uptakes are frequently a topic of discussion during multidisciplinary oncology consultations. The characterization of these uptakes (benign versus malignant) is particularly challenging when considering curative treatment, as rib lesion biopsy is invasive and not always feasible. Their interpretation can significantly impact patient management, potentially shifting the approach from curative to palliative treatment. Additionally, in clinical practice,  $^{68}\text{Ga}$ )Ga-PSMA-11 uptake in the ribs is commonly observed and often associated with benign lesions. In 2020, Chen *et al.* [30] showed that an isolated rib lesion detected by  $^{68}\text{Ga}$ )Ga-PSMA-11 PET/CT at the initial staging of PCa was benign in the majority of cases. The primary aim of this study was to assess whether exclusive rib lesions (single or multiple) detected by  $^{68}\text{Ga}$ )Ga-PSMA-11 PET/CT are most often benign. The secondary objective was to investigate whether any clinical parameters and/or PET/CT imaging characteristics could predict the benign or malignant status of these lesions.

## Methods

### Patient population

This retrospective study was approved by the institutional ethics committee (Comité d'Éthique Hospitalo-Facultaire Universitaire de Liège; reference number 2024/154). We retrospectively included patients with PCa of any tumor stage who had undergone  $^{68}\text{Ga}$ )Ga-PSMA-11 PET/CT for either biochemical recurrence (BCR) or staging and were eligible for treatment with curative intent, that is, radical prostatectomy or external beam radiation therapy (EBRT) to PCa and to pelvic lymph nodes when indicated or stereotactic body radiation therapy (SBRT) to rib lesion(s) after prior treatment to primary PCa (radiotherapy or surgery). Patients who benefited from additional stereotactic radiation therapy to exclusive rib lesions in case of oligometastatic disease were also included. Patients were selected from the  $^{68}\text{Ga}$ )Ga-PSMA-11 PET/CT database of the Nuclear Medicine Department at CHU of Liege from October

2014 to January 2024 using the following keywords: rib(s), costal(s), recurrence, or initial staging. Patients with one or more exclusive rib lesions showing  $^{68}\text{Ga}$ )Ga-PSMA-11 uptake described in the pre-therapeutic  $^{68}\text{Ga}$ )Ga-PSMA-11 PET/CT report, with or without pelvic lymph node, were included. Patients with metastatic disease of other locations than ribs were excluded. To be able to determine the final diagnosis of exclusive rib lesions, benign or malignant, based on the posttherapeutic PSA level, patients with the following management after PSMA PET/CT were excluded: patients who received systemic treatment (hormone therapy or chemotherapy), patients who had a concomitant cancer, patients who received simultaneous therapy to the primary PCa and SBRT directed to exclusive rib lesion(s) at diagnosis, and patients who underwent active surveillance without any treatment. Collected data included clinical and  $^{68}\text{Ga}$ )Ga-PSMA-11 PET/CT characteristics: age, PSA level at imaging, clinical stage, the International Society of Urological Pathology (ISUP) grade group, miT and miN stages (PROMISE V2), the number, location, and CT appearance of rib lesions, and the maximum standardized uptake value of each rib lesion ( $\text{SUV}_{\text{max}}$ ) [31].

### $^{68}\text{Ga}$ )Ga-PSMA-11 PET/CT acquisition

Before February 2022, the  $^{68}\text{Ga}$ )Ga-PSMA-11 PET/CT scans were acquired using GEMINI TF Big Bore or GEMINI TF 16 (Philips, Philips Medical Systems, Cleveland, Ohio, USA) PET/CT systems. After February 2022, PET/CT scans were acquired using a Biograph Vision 600 (Siemens Healthineers, Siemens Healthineers, Knoxville, Tennessee, USA) PET/CT system. Before February 2022, an average activity of 142 MBq (range: 90–166 MBq) of  $^{68}\text{Ga}$ )Ga-PSMA-11 was injected intravenously into the patient. PET images were acquired from the vertex to the inguinal fossae, with the arms placed above the head when possible, on a GEMINI TF Big Bore or a GEMINI TF 16 after a median uptake time of 74 min (range: 47–107 min), with an acquisition time of 60–120 s per bed position, depending on the patient's BMI (50% step overlap). A low-dose CT (3 mm slice thickness, 120 kV tube voltage, and 25 mAs current) was performed for attenuation correction, as well as a thin-slice thoraco-abdomino-pelvic CT [with intravenous (IV) contrast injection if prescribed by the referring physician; 1 mm slice thickness, 120 kV tube voltage, and current ranging from 150 to 250 mAs depending on the patient's BMI]. The thin-slice CT was acquired during breath-hold inspiration. PET images were reconstructed using an iterative method incorporating time-of-flight information and including corrections for attenuation, dead time, and scattered and random events; voxel size was  $4 \times 4 \times 4 \text{ mm}^3$ .

Starting in February 2022, PET images were acquired in a Biograph Vision 600 PET/CT system, after a median uptake time of 66 min (range: 55–95 min) and with an

acquisition speed depending on the anatomical area imaged and the patient's BMI. A total of 1 MBq/kg of [<sup>68</sup>Ga]Ga-PSMA-11 was injected intravenously, with an average injected activity of 92 MBq (range: 71–109 MBq). Patients were positioned as described above. A low-dose CT (2 mm slice thickness, 100 kV tube voltage, and 25 mAs current) was performed for attenuation correction, as well as a thin-slice thoraco-abdomino-pelvic CT (with IV contrast injection if prescribed by the referring physician; 1.5 mm slice thickness, 120 kV tube voltage, and 66 mAs current). The thin-slice CT was acquired during breath-hold inspiration. PET images were reconstructed using an iterative method incorporating time-of-flight information and including corrections for attenuation, dead time, and scattered and random events; voxel size was 1.65 × 1.65 × 1.65 mm<sup>3</sup>. This concerns 26 of our 54 patients (48.1%).

### [<sup>68</sup>Ga]Ga-PSMA-11 PET/CT scan analysis

Based on the description and conclusion of [<sup>68</sup>Ga]Ga-PSMA-11 PET/CT reports, rib lesions were categorized as benign, malignant, or equivocal. The diagnosis was made at the nuclear medicine physician's discretion as part of routine clinical practice, and the SUV<sub>max</sub> or a cutoff value of SUV<sub>max</sub> is not used routinely to distinguish between malignant and benign lesions. All foci of increased activity reported on the rib cage were included. The presence or absence of a CT lesion as reported by a certified radiologist was recorded. Images were retrospectively reviewed by a fifth-year resident, supervised by an experienced nuclear medicine physician. The SUV<sub>max</sub> was retrospectively extracted from a volume of interest (VOI) delineated on the single costal lesion or on the most intense costal lesion in cases of multiple lesions. Following a change of PET/CT system in February 2022 and a decrease in the injected activity into patients, a ratio of the SUV<sub>max</sub> of the most intense costal lesion to the SUV<sub>max</sub> obtained in a 1 cm<sup>3</sup> VOI delineated in the right inferior liver parenchyma was calculated.

Subsequently, the miTN (M0) classification was also performed retrospectively.

### Final classification of rib lesions

All patients were treated with curative intent. The final classification of rib lesions as malignant or benign was based solely on the PSA level measured after the treatment, and the PSA level interpretation depended on the type of treatment. After radical prostatectomy, the rib lesions were classified benign if the PSA was undetectable within 2 months after surgery [4]. If the PSA was detectable after radical prostatectomy, the rib lesions were classified malignant. After EBRT to prostate (with or without pelvic lymph nodes), the rib lesions were defined benign if the PSA nadir was less than 0.5 ng/ml; this level might be reached more slowly, potentially taking up to 3 years or more [4]. Rib lesions were classified

malignant if PSA was detectable after radiation therapy. The PSA nadir after SBRT has not been established. In this study, in cases of rib lesions treated with SBRT, they were considered malignant if PSA was undetectable or reduced after SBRT. Conversely, a rib lesion was considered benign if PSA was stable or progressed after SBRT.

According to the final classification based on the post-therapeutic PSA measurement, benign or malignant rib lesions, the rib lesions described in the report of the PSMA PET/CT were categorized as true positive (TP), true negative (TN), FP, or false negative (FN).

### Statistical analysis

In order to identify whether there were any clinical or PET/CT variables that could have impacted the PET/CT report (benign/equivocal or malignant) on one hand, and on the other hand, to evaluate if any of these variables could be associated with the final benign versus malignant diagnosis, we conducted Student's *t*-test, Mann-Whitney test, and Fisher's exact test.

Quantitative variables were summarized using means and SD, whereas categorical variables were summarized using percentages. Normal distribution of continuous variables was assessed through comparison of means and medians, examination of histograms, quantile-quantile plots, and the Shapiro-Wilk test (normality rejected if *P* < 0.05). Subsequently, paired samples were analyzed using Student's *t*-test. Differences in scores were evaluated with the nonparametric Mann-Whitney test. Categorical data were assessed using Fisher's exact test, as the conditions for applying the chi-square test were not met due to the small sample size. Statistical significance was defined as a *P*-value < 0.05. All statistical analyses were conducted using R Commander software (version 4.3.1; GNU General Public License, Boston, Massachusetts, USA).

## Results

### Patient population

A total of 54 patients were included in the study at initial staging (*N* = 39/54; 72.2%) or at BCR (*N* = 15/54; 27.8%). Patient characteristics are detailed in the supplemental data (Supplementary Table 1, Supplemental digital content 1, <http://links.lww.com/NMC/A309>). PET/CT scans were acquired in a GEMINI TF for 28/54 (51.9%) patients with the Biograph Vision 600 PET/CT system for 26/54 (48.1%). The study flow diagram is presented in Fig. 1.

### Final classification of the rib lesions

In the entire population, rib lesions were benign in 46/54 (85.2%) patients and malignant in 8/54 (14.8%) patients. In the population who benefited from radical prostatectomy (*N* = 37/54; 68.5%), rib lesions were benign (undetectable postoperative PSA) in 34/37 (91.9%) patients and

Fig. 1

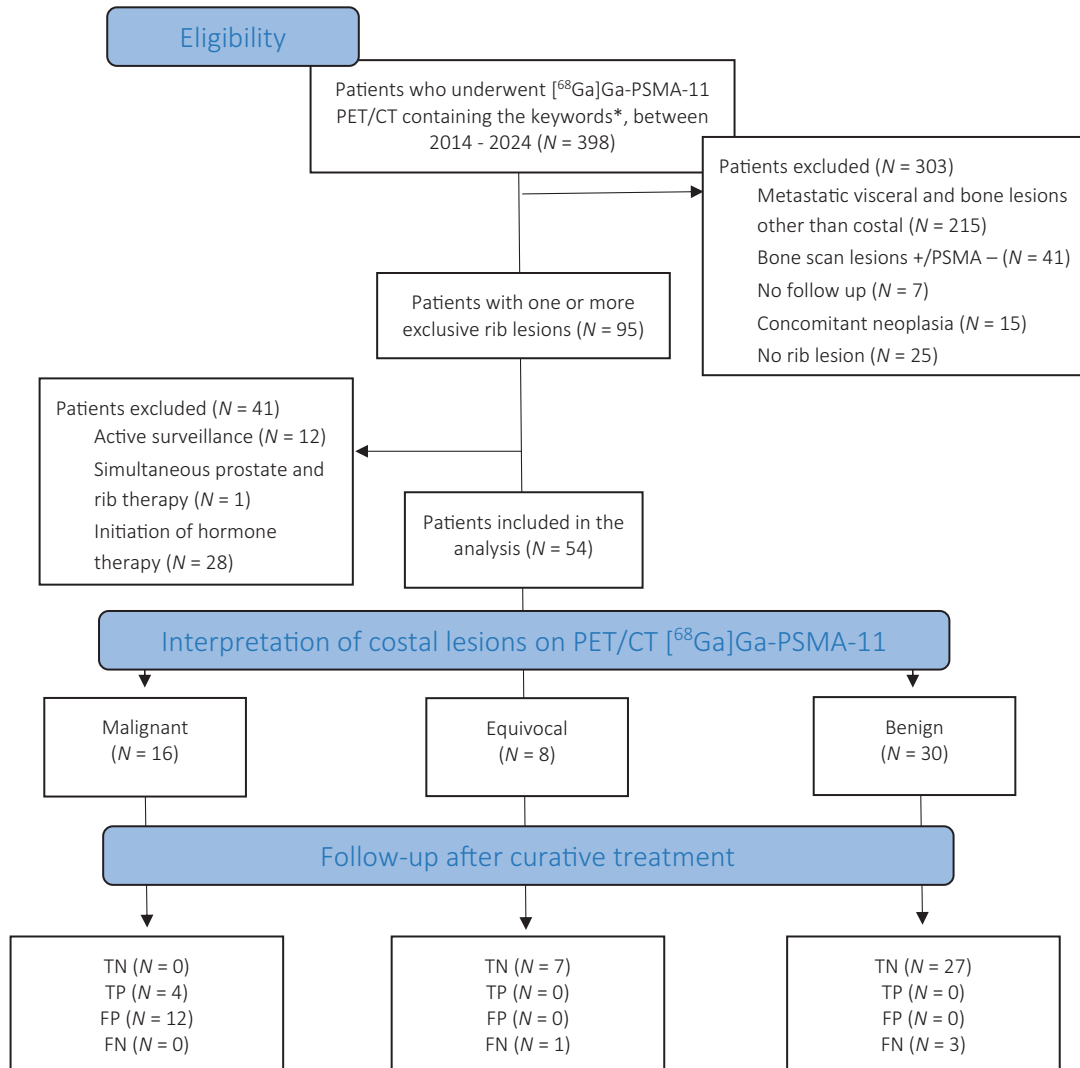


Diagram of the selection and classification of the 54 patients included in this work. \*Keywords used in the search: rib(s), costal(s), recurrence, and initial staging. CT, computed tomography; FN, false negative; FP, false positive;  $^{68}\text{Ga}$ ]Ga-PSMA-11,  $^{68}\text{Ga}$  Gallium-labelled prostate-specific membrane antigen; PSMA, prostate-specific membrane antigen; TN, true negative; TP, true positive.

malignant (detectable postoperative PSA) in 3/37 (8.1%) patients. In the population who benefited from radiation therapy ( $N = 12/54$ ; 22.2%), rib lesions were benign (PSA nadir  $< 0.5$  ng/ml) in 9/12 (75%) patients and malignant (PSA nadir  $\geq 0.5$  ng/ml) in 3/12 (25%) patients. In the population who benefited from stereotactic body radiation therapy ( $N = 5/54$ ; 9.3%), rib lesions were classified benign in 3/5 (60%) patients and malignant in 2/5 (40%) patients.

#### PET/CT $^{68}\text{Ga}$ ]Ga-PSMA-11 scan analysis

Among the 54 patients included in the study, a total number of 74 costal foci with  $^{68}\text{Ga}$ ]Ga-PSMA-11 uptake were described. The median (range) number of exclusive costal lesions per patient was 1.4 (1–8); a single rib lesion was

described in 44 (81.5%) patients, and multiple rib lesions were visualized in 10 (18.5%) patients. PET/CT characteristics are presented in Supplementary Table 2, Supplemental digital content 1, <http://links.lww.com/NMC/A309>. No patient presenting with exclusive costal foci had other suspicious sites of recurrence, whether local or distant.

The comparison between the PSMA PET/CT report and the final diagnosis after curative treatment is presented in the contingency Table 1, in which benign and equivocal reports were combined. Of 54 patients, 30 (55.6%) were reported to have benign rib lesions ( $N = 34$  rib foci), with a single rib lesion in 28/30 (93.3%) and multiple rib lesions in 2/30 (6.7%). Among these, 27/30 (90%) were confirmed as nonmetastatic (TN), whereas 3/30 (10%) were metastatic (FN). Eight patients (14.8%) had

**Table 1** Proportion of rib lesions reported as benign/equivocal or malignant versus proportion of costal lesions considered benign or malignant based on posttreatment PSA level

	Final diagnosis		Total
	Benign	Malignant	
PSMA PET/CT report			
Described benign/equivocal	34 (63% TN)	4 (7.4% FN)	38 (70.4%)
Described malignant	12 (22.2% FP)	4 (7.4% TP)	16 (29.6%)
Total	46 (85.2%)	8 (14.8%)	54 (100%)

FN, false negative; FP, false positive; PSA, prostate-specific antigen; PSMA PET/CT, prostate-specific membrane antigen PET combined with computed tomography; TN, true negative; TP, true positive.

equivocal costal lesions [ $N = 9$  rib foci; single rib lesion in 7/8 (87.5%) patients and multiple rib lesions in 1/8 (12.5%) patients], of which only one was confirmed to be malignant. Among the 16 patients (29.6%) reported to have malignant costal lesions [ $N = 31$  rib foci; single rib lesion in 9/16 (56.25%) patients and multiple rib lesions in 7/16 (43.75%) patients], four patients were confirmed to be metastatic (TP).

#### Association of clinical and imaging variables with the final diagnosis

The clinical and PET/CT variables tested in patients with a final diagnosis of benign or malignant rib lesions are provided in Table 2. The only variable statistically significantly associated with the final classification of benign or malignant costal lesions was the radiological CT scan report made by the radiologist, categorizing lesions as no visible lesion, benign, or malignant ( $P = 0.0143$ ). When the radiologist reported benign rib lesion(s) in the CT images and the PET/CT scan was reported benign, the final diagnosis was benign in 100% of cases (TN). By contrast, when the radiologist reported the presence of malignant rib lesion(s) in CT images and the PET/CT scan was consequently reported malignant, the final diagnosis was benign in 5/8 (62.5%) of cases (FP).

#### Association of clinical and imaging variables with the conclusion of the PET/CT report

The clinical and PET/CT variables tested among the patients with a PET/CT report of benign ( $N = 30/54$ ; 55.6%) and equivocal ( $N = 8/54$ ; 14.8%) or malignant ( $N = 16/54$ ; 29.6%) rib lesions are presented in Table 3. Statistically significant differences were found for patient age ( $P = 0.0078$ ), rib lesion dispersion ( $P = 0.0044$ ), presence or absence of lesion on CT images ( $P = 0.0001$ ), and SUV<sub>max</sub> of the digital PET/CT system ( $P = 0.0369$ ) across the three types of conclusions in the PSMA PET/CT report (benign, equivocal, malignant).

A subanalysis showed that none of the clinical or imaging parameters were significantly associated with TN, FN, or FP results while patient age was significantly higher in the TP fraction ( $P = 0.0309$ ). Additionally, the study explored whether the nuclear medicine physician who performed the PET/CT protocol had an impact. Supplementary Tables 3 and 4, Supplemental digital

content 1, <http://links.lww.com/NMC/A309>, show the proportions of patients categorized with benign, equivocal, or malignant rib lesions by each physician and the proportions of TN, FN, TP, and FP results for each physician, respectively. Due to the small sample size and the high number of physicians, statistical analyses could not be carried out.

#### Discussion

This study aimed to better characterize exclusive unspecific rib uptake on [<sup>68</sup>Ga]Ga-PSMA-11 PET/CT, a frequent clinical challenge, and to identify criteria to differentiate between benign and malignant cases. Our findings align with Chen and colleague, and a recent systematic review on UBUs of PSMA-targeted radioligands, showing that rib lesions on PSMA PET/CT are often benign [28,30]. This observation can enhance diagnostic confidence, potentially reducing unnecessary biopsies and improving patient management. Specifically, we found that exclusive rib lesions detected by [<sup>68</sup>Ga]Ga-PSMA-11 PET/CT at initial PCa staging or in cases of recurrence were predominantly benign ( $N = 46/54$ ; 85.2%; 95% confidence interval (CI): 75.5–94.5%). This finding supports the observations by Chen *et al.* [30], who reported that a solitary costal lesion on [<sup>68</sup>Ga]Ga-PSMA-11 PET/CT performed at initial staging of PCa patients was benign in the majority of cases ( $N = 61/62$ ; 98.4%; 95% CI: 94.7–100%). The lower proportion of nonmetastatic cases in our study could be attributed to differences in patient inclusion criteria. Our cohort comprised patients with BCR or persistent PSA after curative treatment ( $N = 15/54$ ; 27.8%). In our population, a significant number of patients ( $N = 16/54$ ; 29.6%) were classified as high risk. In contrast, details on the European Association of Urology (EAU) risk categories were not specified in Chen *et al.*, and their patient characteristics differed in terms of PSA levels and Gleason scores. This could explain the distinct prevalence of metastases in the two series. Interestingly, Zacho *et al.* [32] reported that [<sup>68</sup>Ga]Ga-PSMA-11 PET/CT was FP in the skeleton in only 4/112 patients newly diagnosed intermediate- to high-risk PCa, and all four cases were solitary rib lesions. They caution that PSMA-positive solitary costal lesions, with no other positive lesions besides those in the prostate, should be interpreted carefully [32]. Like

**Table 2** Variables of patients with one or more rib lesions with the final diagnosis of benign rib lesions ( $N = 46$ ) and malignant rib lesions ( $N = 8$ )

	Benign rib lesions ( $N = 46$ )	Malignant rib lesions ( $N = 8$ )
<b>Clinical features</b>		
Age (mean $\pm$ SD) (years)	70 $\pm$ 7	73 $\pm$ 10
PSA level on imaging (mean $\pm$ SD) (ng/ml)		
Initial workup ( $N = 39$ )	13.10 $\pm$ 8.20	13.80 $\pm$ 8.20
Biochemical recurrence ( $N = 15$ )	0.41 $\pm$ 0.50	2.29 $\pm$ 3.47
<b>Clinical stage</b>		
T1–T2a	26 (56.6%)	3 (37.5%)
T2b	7 (15.2%)	2 (25%)
T2c	3 (6.5%)	1 (12.5%)
Missing data	10 (21.7%)	2 (25%)
<b>ISUP grade group at the time of diagnosis</b>		
1	7 (15.2%)	2 (25%)
2	19 (41.3%)	1 (12.5%)
3	10 (21.7%)	2 (25%)
4	4 (8.7%)	1 (12.5%)
5	5 (10.9%)	1 (12.5%)
Missing data	1 (2.2%)	1 (12.5%)
<b>EAU risk groups</b>		
Low-risk localized disease	4 (8.7%)	2 (25%)
Intermediate-risk disease	29 (63%)	3 (37.5%)
High-risk disease <sup>a</sup>	13 (28.3%)	3 (37.5%)
<b>[<sup>68</sup>Ga]Ga-PSMA-11 PET/CT parameters</b>		
Number of rib lesions (mean $\pm$ SD)	1.40 $\pm$ 1.20	1.25 $\pm$ 1.00
<b>Lesion dispersion</b>		
Unique ( $N = 44$ )	38 (82.6%)	6 (75%)
Scattered ( $N = 8$ )	6 (13%)	2 (25%)
Aligned ( $N = 2$ )	2 (4.4%)	0 (0%)
<b>Appearance of underlying CT images*</b>		
No lesion ( $N = 31$ )	27 (58.7%)	4 (50%)
Benign lesion ( $N = 14$ )	14 (30.4%)	0 (0%)
Malignant lesion ( $N = 9$ )	5 (10.9%)	4 (50%)
<b>SUV<sub>max</sub> (mean <math>\pm</math> SD)</b>		
Analog PET/CT	2.90 $\pm$ 0.90	7.80 $\pm$ 9.00
Digital PET/CT	2.90 $\pm$ 1.00	2.70 $\pm$ 0.70
Ratio SUV <sub>max</sub> (mean $\pm$ SD)	0.45 $\pm$ 0.23	0.78 $\pm$ 0.90
<b>miT (initial workup; <math>N = 39</math>)</b>		
miT2u	8/35 (22.9%)	1/4 (25%)
miT2m	26/35 (74.3%)	3/4 (75%)
miT3	1/35 (2.8%)	0/4 (0%)
<b>miN (initial workup; <math>N = 39</math>)<sup>b</sup></b>		
miN0	33/35 (94.3%)	4/4 (100%)
miN1a	1/35 (2.85%)	0/4 (0%)
miN1b	1/35 (2.85%)	0/4 (0%)

CT, computed tomography; EAU, European Association of Urology; [<sup>68</sup>Ga]Ga-PSMA-11, <sup>68</sup>Gallium-labelled prostate-specific membrane antigen; ISUP, International Society of Urological Pathology; PET/CT, PET combined with computed tomography; PSA, prostate-specific antigen; SUV<sub>max</sub>, maximum standardized uptake value.

<sup>a</sup>High-risk localized disease/locally advanced disease.

<sup>b</sup>The statistical test was not performed for the miN due to the low number of miN1a/b.

\*Statistically significant results ( $P < 0.05$ ).

Chen *et al.* [30], our study included cases where benign costal lesions were associated with fractures in the CT images ( $N = 3/54$ ; 5.6%). In our population, 2 of 39 (5.1%) patients for whom the PSMA PET/CT was performed for staging had low-risk localized disease. The EAU recommendation is to not use additional imaging for staging purposes in patients with low-risk localized disease [4]. However, in these two patients, conventional imaging was performed and resulted in equivocal results, triggering the performance of PSMA PET/CT, which showed

the absence of metastatic disease. This emphasizes the misuse of imaging and potential FP resulting in unnecessary or expensive additional tests. Of note, a bone scan was conducted in eight patients before PSMA PET/CT. It also revealed suspicious rib foci, which led to the decision to proceed with PSMA PET/CT.

This study highlights the pitfalls associated with [<sup>68</sup>Ga]Ga-PSMA-11 PET/CT. While known, these pitfalls have not been extensively documented in publications that demonstrate the predominantly benign nature of exclusive rib lesions [13,32]. In contrast, other tracers such as [<sup>18</sup>F]PSMA-1007 and [<sup>18</sup>F]rhPSMA-7 have shown high rates of UBUs [15,18–28]. These tracers often show focal uptake without an apparent underlying lesion on CT images, and the reasons for this costal fixation remain unclear. One theory suggests that the lower positron energy of [<sup>18</sup>F] compared with [<sup>68</sup>Ga] provides better spatial resolution, whereas the longer half-life of [<sup>18</sup>F] enhances the signal-to-noise ratio, potentially explaining the higher incidence of ribs UBUs [18,19,28]. PSMA expression in inflammatory tissues and neovessels of angiogenesis may also contribute to these observations, particularly in regions rich in bone marrow like the ribs and pelvis [18,19]. The exact reason why ribs are a common site for radiotracer uptake remains uncertain [18,19]. These findings are crucial for managing patients with exclusive costal lesions, as many of these lesions are non-metastatic and should not preclude potential curative treatment. Figures 2–4 illustrate representative cases.

In our study, we investigated whether clinical factors (PSA level, patient age, ISUP grade group, cT stage) and/or PSMA PET/CT characteristics (SUV<sub>max</sub>, SUV<sub>max</sub> ratio, presence of lesion on CT images, scatter of costal lesions, number of costal lesions, and miT and miN stages) could help avoid FP or FN diagnoses (Table 2). When comparing patients with benign versus malignant costal lesions, only the appearance on CT scans showed a significant difference between the two groups ( $P = 0.0143$ ). Specifically, when CT scans indicated a benign lesion associated with the costal PSMA-positive focus in the PET images, the diagnosis was correct in all cases ( $N = 14/14$ ; 100%; no false negative case). In contrast, among patients with radiologically suspicious costal lesions, only 44.4% ( $N = 4/9$ ) were confirmed to be malignant, while the remaining 5/9 patients had benign costal lesions (55.6% FP cases). These findings underscore the importance of careful interpretation of radiological appearances associated with costal PSMA-positive foci, as they can sometimes be misleading.

Following this, we investigated whether the same clinical and [<sup>68</sup>Ga]Ga-PSMA-11 PET/CT image characteristics influenced the PET/CT reports (Table 3). Patient age was significantly higher among patients classified as metastatic ( $P = 0.078$ ). We hypothesize that advanced age may contribute to costal uptake related to

**Table 3** Variables of patients with rib lesions reported benign (*N* = 30), malignant (*N* = 16), or equivocal (*N* = 8) in the [<sup>68</sup>Ga]Ga-PSMA-11 reports

	Rib lesions reported benign ( <i>N</i> = 30)	Rib lesions reported equivocal ( <i>N</i> = 8)	Rib lesions reported malignant ( <i>N</i> = 16)
<b>Clinical features</b>			
Age* (mean ± SD) (years)	68 ± 6	71 ± 9	74 ± 7
PSA level at imaging (mean ± SD) (ng/ml)			
Initial work up	12.39 ± 7.20	14.16 ± 7.03	14.65 ± 11.20
Biochemical recurrence	0.35 ± 0.34	2.63 ± 4.19	0.56 ± 0.60
<b>Clinical stage</b>			
T1–T2a	14 (46.7%)	4 (50%)	11 (68.8%)
T2b	7 (23.3%)	1 (12.5%)	1 (6.2%)
T2c	3 (10%)	1 (12.5%)	0 (0%)
Missing data	6 (20%)	2 (25%)	4 (25%)
<b>ISUP grade group at the time of diagnosis</b>			
1	5 (16.7%)	0 (0%)	4 (25%)
2	10 (33.3%)	4 (50%)	6 (37.5%)
3	8 (26.7%)	1 (12.5%)	3 (18.75%)
4	1 (3.3%)	1 (12.5%)	3 (18.75%)
5	5 (16.7%)	1 (12.5%)	0 (0%)
Missing data	1 (3.3%)	1 (12.5%)	0 (0%)
<b>EAU risk groups</b>			
Low-risk localized disease	3 (10%)	0 (0%)	3 (18.7%)
Intermediate-risk disease	19 (63.3%)	5 (62.5%)	8 (50%)
High-risk disease <sup>a</sup>	8 (26.7%)	3 (37.5%)	5 (31.3%)
<b>[<sup>68</sup>Ga]Ga-PSMA-11 PET/CT parameters</b>			
Number of rib lesions (mean ± SD)	1.13 ± 0.57	1.13 ± 0.35	1.94 ± 1.81
<b>Lesion dispersion*</b>			
Unique ( <i>N</i> = 44)	28 (93.3%)	7 (87.5%)	9 (56.3%)
Scattered ( <i>N</i> = 8)	2 (6.7%)	1 (12.5%)	5 (31.2%)
Aligned ( <i>N</i> = 2)	0 (0%)	0 (0%)	2 (12.5%)
<b>Appearance of underlying CT images*</b>			
No lesion ( <i>N</i> = 31)	16 (53.3%)	7 (87.5%)	8 (50%)
Benign lesion ( <i>N</i> = 14)	14 (46.7%)	0 (0%)	0 (0%)
Malignant lesion ( <i>N</i> = 9)	0 (0%)	1 (12.5%)	8 (50%)
<b>SUV<sub>max</sub> (mean ± SD)</b>			
Analog PET/CT	2.8 ± 0.9	2.8 ± 0.7	4.8 ± 5.6
Digital PET/CT*	2.6 ± 0.6	3.1 ± 1.1	3.9 ± 0.6
Ratio SUV <sub>max</sub> (mean ± SD)	0.41 ± 0.10	0.45 ± 0.26	0.69 ± 0.69
<b>miT (initial workup) (<i>N</i> = 39)</b>			
miT2u	7/25 (28%)	1/5 (20%)	1/9 (11.1%)
miT2m	17/25 (68%)	4/5 (80%)	8/9 (88.9%)
miT3	1/25 (4%)	0/5 (0%)	0/9 (0%)
<b>miN (initial workup) (<i>N</i> = 39)<sup>b</sup></b>			
miN0	14/25 (56%)	5/5 (100%)	9/9 (100%)
miN1a	1/25 (4%)	0 (0%)	0 (0%)
miN1b	1/25 (4%)	0 (0%)	0 (0%)

CT, computed tomography; EAU, European Association of Urology; [<sup>68</sup>Ga]Ga-PSMA-11, <sup>68</sup>Gallium-labelled prostate-specific membrane antigen; ISUP, International Society of Urological Pathology; PET/CT, PET combined with computed tomography; PSA, prostate-specific antigen; SUV<sub>max</sub>, maximum standardized uptake value.

<sup>a</sup>High-risk localized disease/locally advanced disease.

<sup>b</sup>The statistical test was not performed for the miN due to the low number of miN1a/b.

\*Statistically significant results (*P* < 0.05).

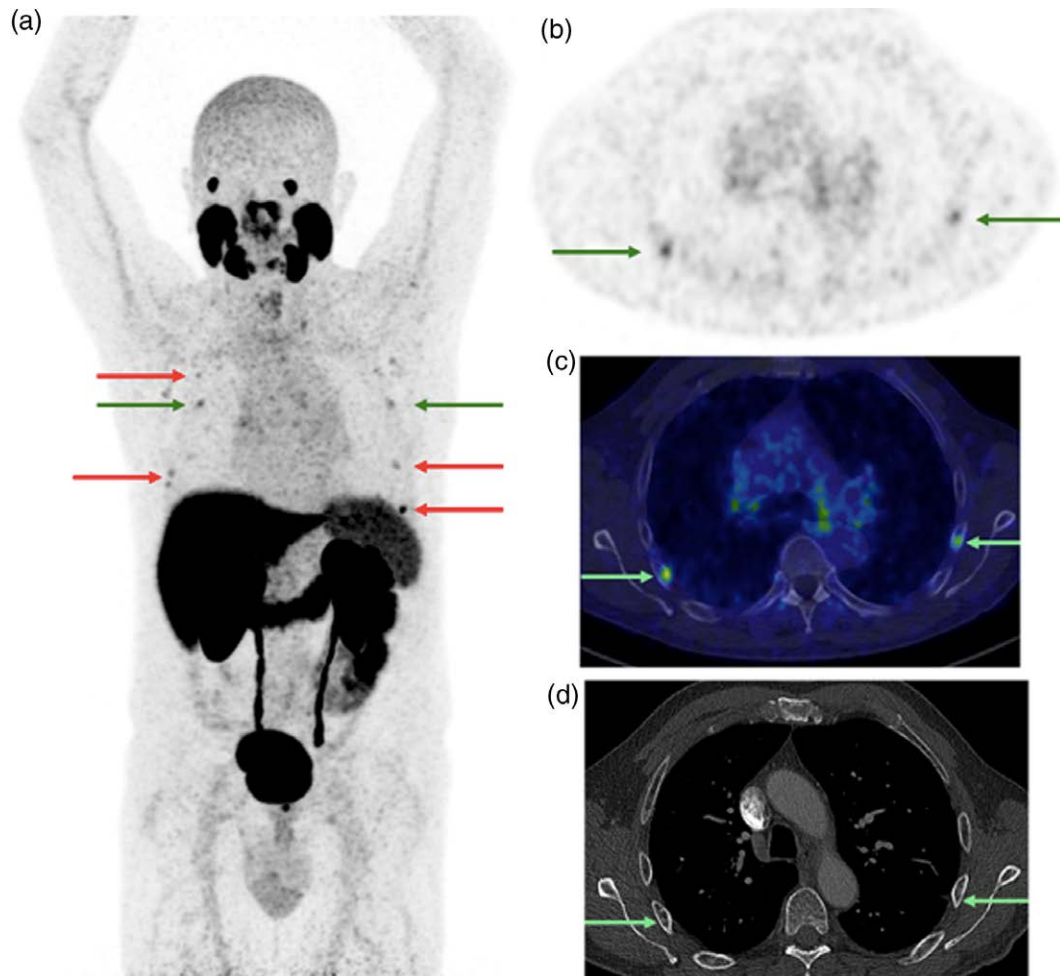
microfractures associated with osteopenia/osteoporosis, which increases with age. The SUV<sub>max</sub> of the hottest costal focus measured on digital PET/CT was significantly higher in patients with rib lesions classified as malignant (*P* = 0.0369), whereas the SUV<sub>max</sub> extracted from PET images acquired on the analog PET/CT system showed wide variation (mean ± SD SUV<sub>max</sub> 4.8 ± 5.6) and no significant association with the PET/CT report.

Radiological appearance (presence or not of a lesion on CT images) and lesion dispersion (single versus scattered) differed significantly among the three types of PET/CT reports (*P* = 0.0044). The influence of the CT

appearance of rib lesion on the final diagnosis of PET/CT has been discussed earlier.

Additionally, single costal lesions were more likely to be classified as benign, whereas multiple scattered lesions were often classified as malignant. This study also indicates variability depending on the nuclear medicine physician. Notably, half of the false-positive results were attributed to the same nuclear medicine physician (Supplementary Table 4, Supplemental digital content 1, <http://links.lww.com/NMC/A309>). Due to limited variables that reliably distinguish between benign and malignant lesions, when there is uncertainty about whether

Fig. 2



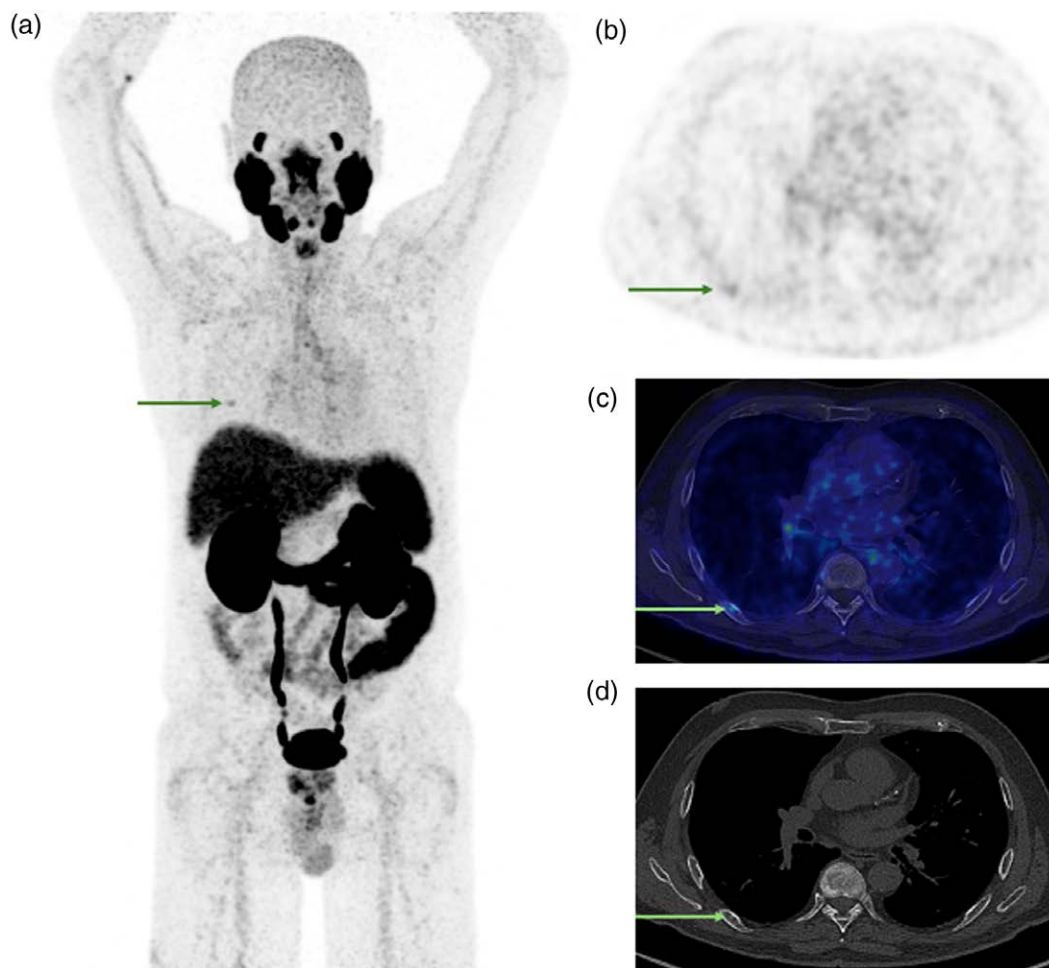
[ $^{68}\text{Ga}$ ]Ga-PSMA-11 PET/CT images [PET maximum intensity projection and transverse slice showing rib foci indicated by arrows (a) and (b); fused PET/low dose CT (c); and diagnostic contrast-enhanced CT (d); PET SUV scale 0–5; date: May 2022] of a 70-year-old patient who undergone initial staging for PCa (PSA level 9.06 ng/ml at the time of imaging; clinical stage cT1a; ISUP grade group 4). The PET/CT scan revealed multiple costal lesions (arrows) interpreted as malignant based on CT appearance (sclerotic bone lesions), with stage miT2mNOM1b and  $\text{SUV}_{\text{max}}$  of the most intense costal lesion of 5.9. Based upon the decision of the multidisciplinary oncology consultation, a bone biopsy was performed on the most intense costal lesion, yielding a negative result. This led to the conclusion that the PSMA PET/CT results were false positive. Subsequently, a radical prostatectomy with pelvic lymph node dissection was performed. The pathological stage was pT2N0 and the postoperative PSA was undetectable, confirming false positive rib lesions described by the PSMA PET/CT. CT, computed tomography; [ $^{68}\text{Ga}$ ]Ga-PSMA-11,  $^{68}\text{Ga}$  Gallium-labelled prostate-specific membrane antigen; ISUP, International Society of Urological Pathology; PSA, prostate-specific antigen; PSMA, prostate-specific membrane antigen;  $\text{SUV}_{\text{max}}$ , maximum standardized uptake value.

a lesion is malignant, a CT-guided rib biopsy should be considered whenever feasible. In this study, two of the 54 included patients underwent rib biopsy, which resulted in negative pathological findings. Despite its invasiveness and associated risks such as pneumothorax, rib biopsy has shown high effectiveness, providing an accurate diagnosis in a significant majority of cases (88%) [33]. Indeed, a reliable diagnosis and accurate interpretation of PSMA PET/CT scans, avoiding the description of falsely malignant lesions, are crucial for patients, especially when curative treatment is an option.

One major limitation of our study is the exclusion of patients with one or more exclusive costal lesions who

undergone hormone therapy ( $N = 28/95$ ; 29.5%). Due to our stringent inclusion criteria required to be able to determine the final diagnosis of rib lesions as benign or malignant based on the posttherapeutic PSA level, we could not include these patients in the study. This may have introduced a bias, as it is possible that additional metastatic rib lesions could be found in this group. Similar to the group with a strong gold standard, radiological features might be helpful, though, as 6/28 (21.4%) had definitive benign lesions on the low-dose CT, and 11/28 (39.3%) had CT features which, combined with the clinical data, decided the clinicians to treat the patients with stereotactic costal radiotherapy (combined with

Fig. 3



[<sup>68</sup>Ga]Ga-PSMA-11 PET/CT images [PET maximum intensity projection and transverse slice showing rib focus indicated by arrows (a) and (b); fused PET/low dose CT (c); and diagnostic noncontrast-enhanced CT (d); PET SUV scale 0–5; date: March 2022] of a 69-year-old patient who undergone initial staging for PCa (PSA level 15.48 ng/ml at the time of imaging; clinical stage cT1a; ISUP grade group 1). The PET/CT scan revealed a solitary costal lesion (arrows) interpreted as benign based on CT appearance (fibrous dysplasia), with stage mT2mN0M0 and SUV<sub>max</sub> of the costal lesion of 2.5. Subsequently, a radical prostatectomy with pelvic lymph node dissection was performed. The pathological stage was pT3aN0 and the postoperative PSA was undetectable, confirming true negative rib lesion described by the PSMA PET/CT. CT, computed tomography; [<sup>68</sup>Ga]Ga-PSMA-11, <sup>68</sup>Gallium-labelled prostate-specific membrane antigen; PCa, prostate cancer; PSA, prostate-specific antigen; PSMA, prostate-specific membrane antigen; SUV<sub>max</sub>, maximum standardized uptake value.

hormonal therapy). That leaves 11 patients with undetermined lesions and who received hormone therapy. All were intermediate or high-risk PCa, and caution should be exercised in these patients, before neglecting undetermined multiple rib lesions. Currently, there are no definitive recommendations for managing oligometastatic patients, but targeted treatment of metastases without immediate hormone therapy appears to offer promising outcomes in terms of progression-free survival, while potentially reducing toxicity. Phase III studies are ongoing to assess the impact on overall survival in these patients [34].

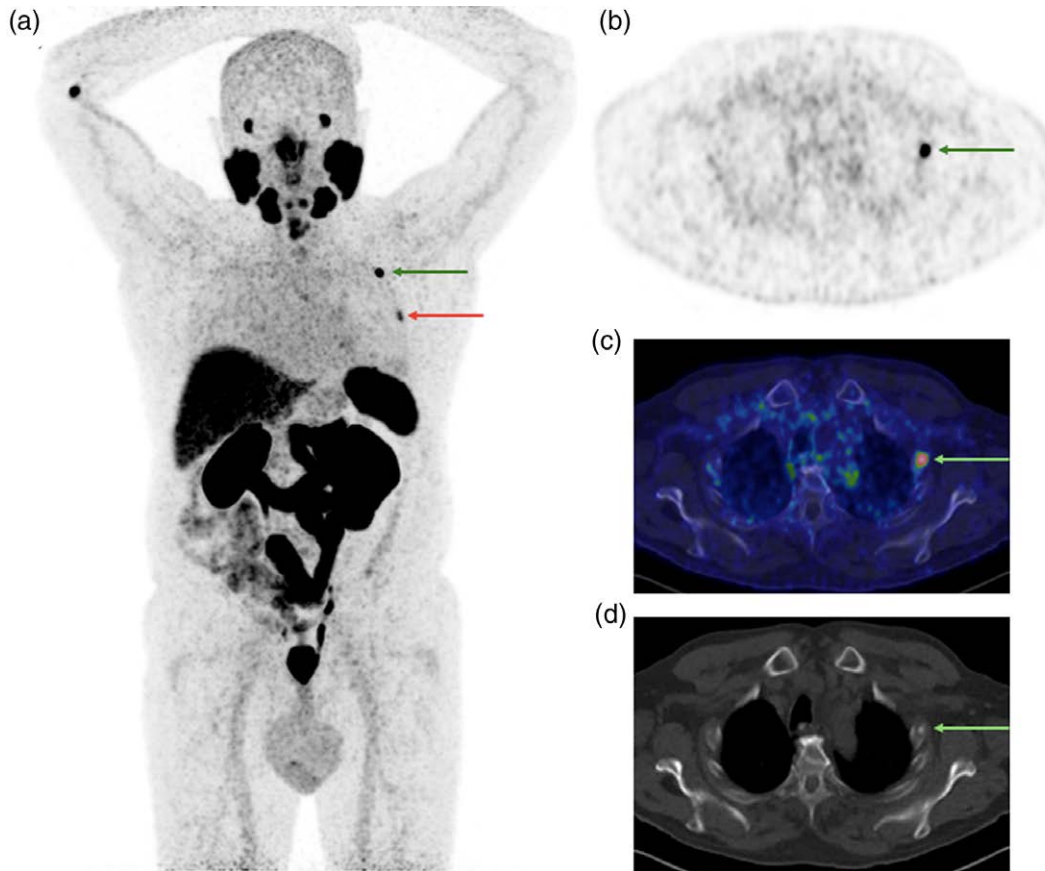
Our study also has other limitations, as it is retrospective in nature. We elected not to review the PET and

CT images, as to evaluate the “real-world” clinical performances of the technique. The first PET/CT scans were reported in 2014, predating the awareness of PSMA PET/CT pitfalls described later in the literature [13–17,35]. Also, the sample size of included patients remains small, but that probably reflects the reduced proportion of PCa patients with bone lesions limited to the ribs.

### Conclusion

This study confirms that when one or more exclusive costal lesions are identified using [<sup>68</sup>Ga]Ga-PSMA-11 PET/CT during initial staging or in cases of BCR after curative treatment for PCa, these lesions are

Fig. 4



[<sup>68</sup>Ga]Ga-PSMA-11 PET/CT images [PET maximum intensity projection and transverse slice showing rib foci indicated by arrows (a and b); fused PET/low-dose CT (c); and diagnostic noncontrast-enhanced CT (d); PET SUV scale 0–5; date: October 2023] of a 75-year-old patient who undergone biochemical recurrence for PCa (PSA level 0.17 ng/ml at the time of imaging; clinical stage cT1a; ISUP grade group 3). The PET/CT scan revealed two costal lesions (arrows) interpreted as malignant based on CT appearance (sclerotic lesions), with stage mTrON0M1b and SUV<sub>max</sub> of the most intense costal lesion of 21.4. Subsequently, SBRT to both rib lesions was performed. Posttreatment PSA was undetectable, confirming true positive rib lesions described by the PSMA PET/CT. CT, computed tomography; [<sup>68</sup>Ga]Ga-PSMA-11, <sup>68</sup>Gallium-labelled prostate-specific membrane antigen; PCa, prostate cancer; PSA, prostate-specific antigen; PSMA, prostate-specific membrane antigen; SBRT, stereotactic body radiation therapy; SUV<sub>max</sub>, maximum standardized uptake value.

predominantly benign. Furthermore, the study highlights that no clinical or PET/CT feature reliably distinguishes between benign and metastatic costal lesions, except for specific benign CT features that reliably differentiate benign from metastatic costal lesions.

### Acknowledgement

The authors express their appreciation to Justine Monseur from the Department of Public Health Sciences Biostatistics, CHU de Liège, for supervising and providing statistical data.

### Conflicts of interest

There are no conflicts of interest.

### References

- Cornford P, van den Bergh RCN, Briers E, Van den Broeck T, Brunckhorst O, Darraugh J, *et al.* EAU-EANM-ESTRO-ESUR-ISUP-SIOG guidelines on prostate cancer – 2024 update. Part I: screening, diagnosis, and local treatment with curative intent. *Eur Urol* 2024; **86**:148–163.
- Bray F, Laversanne M, Sung H, Ferlay J, Siegel RL, Soerjomataram I, Jemal A. Global cancer statistics 2022: GLOBOCAN estimates of incidence and mortality worldwide for 36 cancers in 185 countries. *CA Cancer J Clin* 2024; **74**:229–263.
- Global Cancer Observatory (GCO). *Data visualization tools for exploring the global cancer burden in 2022*. 2022. <https://gco.iarc.fr/today/home>. [Accessed 24 April 2024]
- Cornford P, Tilki D, van den Bergh RCN, Briers E, Santis MD, Fanti S, *et al.* EAU-EANM-ESTRO-ESUR-ISUP-SIOG guidelines on prostate cancer. European Association of Urology Guidelines Office; 2024.
- Hövels AM, Heesakkers RAM, Adang EM, Jager GJ, Strum S, Hoogeveen YL, *et al.* The diagnostic accuracy of CT and MRI in the staging of pelvic lymph nodes in patients with prostate cancer: a meta-analysis. *Clin Radiol* 2008; **63**:387–395.
- Alipour R, Azad A, Hofman MS. Guiding management of therapy in prostate cancer: time to switch from conventional imaging to PSMA PET? *Ther Adv Med Oncol* 2019; **11**:1758835919876828.
- Hofman MS, Lawrentschuk N, Francis RJ, Tang C, Vela I, Thomas P, *et al.*; proPSMA Study Group Collaborators. Prostate-specific membrane antigen PET-CT in patients with high-risk prostate cancer before curative-intent surgery or radiotherapy (proPSMA): a prospective, randomised, multicentre study. *Lancet* 2020; **395**:1208–1216.

- 8 Emmett L, Buteau J, Papa N, Moon D, Thompson J, Roberts MJ, et al. The additive diagnostic value of prostate-specific membrane antigen positron emission tomography computed tomography to multiparametric magnetic resonance imaging triage in the diagnosis of prostate cancer (PRIMARY): a prospective multicentre study. *Eur Urol* 2021; **80**:682–689.
- 9 Jeet V, Parkinson B, Song R, Sharma R, Hoyle M. Histopathologically validated diagnostic accuracy of PSMA-PET/CT in the primary and secondary staging of prostate cancer and the impact of PSMA-PET/CT on clinical management: a systematic review and meta-analysis. *Semin Nucl Med* 2023; **53**:706–718.
- 10 Jadvar H, Calais J, Fanti S, Feng F, Greene KL, Gulley JL, et al. Appropriate use criteria for prostate-specific membrane antigen PET imaging. *J Nucl Med* 2022; **63**:59–68.
- 11 Perera M, Papa N, Roberts M, Williams M, Udovicich C, Vela I, et al. Gallium-68 prostate-specific membrane antigen positron emission tomography in advanced prostate cancer – updated diagnostic utility, sensitivity, specificity, and distribution of prostate-specific membrane antigen-avid lesions: a systematic review and meta-analysis. *Eur Urol* 2019; **77**:403–417.
- 12 Wong SK, Mohamad NV, Giaze TR, Chin K, Mohamed N, Ima-Nirwana S. Prostate cancer and bone metastases: the underlying mechanisms. *Int J Mol Sci* 2019; **20**:2587.
- 13 Sheikhbahaei S, Afshar-Oromieh A, Eiber M, Solnes LB, Javadi MS, Ross AE, et al. Pearls and pitfalls in clinical interpretation of prostate-specific membrane antigen (PSMA)-targeted PET imaging. *Eur J Nucl Med Mol Imaging* 2017; **44**:2117–2136.
- 14 Sheikhbahaei S, Werner RA, Solnes LB, Pienta KJ, Pomper MG, Gorin MA, Rowe SP. Prostate-specific membrane antigen (PSMA)-targeted PET imaging of prostate cancer: an update on important pitfalls. *Semin Nucl Med* 2019; **49**:255–270.
- 15 Rauscher I, Krönke M, König M, Gafita A, Maurer T, Horn T, et al. Matched-pair comparison of <sup>68</sup>Ga-PSMA-11 PET/CT and <sup>18</sup>F-PSMA-1007 PET/CT: frequency of pitfalls and detection efficacy in biochemical recurrence after radical prostatectomy. *J Nucl Med* 2020; **61**:51–57.
- 16 Merrild EH, Baerentzen S, Bouchelouche K, Buus S. Vertebral myeloma mimicking prostatic carcinoma metastasis in <sup>68</sup>Ga-PSMA PET/CT. *Clin Nucl Med* 2017; **42**:790–792.
- 17 Muselaers S, Erdem S, Bertolo R, Ingels A, Kara O, Pavan N, et al; On Behalf of the European Association Of Urology EAU Young Academic Urologists YAU Renal Cancer Working Group. PSMA PET/CT in renal cell carcinoma: an overview of current literature. *J Clin Med* 2022; **11**:1829.
- 18 Seifert R, Telli T, Opitz M, Barbato F, Berliner C, Nader M, et al. Unspecific <sup>18</sup>F-PSMA-1007 bone uptake evaluated through PSMA-11 PET, bone scanning, and MRI triple validation in patients with biochemical recurrence of prostate cancer. *J Nucl Med* 2023; **64**:738–743.
- 19 Grunig H, Maurer A, Thal Y, Kovacs Z, Strobel K, Burger IA, Müller J. Focal unspecific bone uptake on [<sup>18</sup>F]-PSMA-1007 PET: a multicenter retrospective evaluation of the distribution, frequency, and quantitative parameters of a potential pitfall in prostate cancer imaging. *Eur J Nucl Med Mol Imaging* 2021; **48**:4483–4494.
- 20 Dietlein F, Kobe C, Hohberg M, Zlatopolskiy BD, Krapf P, Endepols H, et al. Intraindividual comparison of <sup>18</sup>F-PSMA-1007 with renally excreted PSMA ligands for PSMA PET imaging in patients with relapsed prostate cancer. *J Nucl Med* 2020; **61**:729–734.
- 21 Arnfield EG, Thomas PA, Roberts MJ, Pelecanos AM, Ramsay SC, Lin CY, et al. Clinical insignificance of [<sup>18</sup>F]PSMA-1007 avid non-specific bone lesions: a retrospective evaluation. *Eur J Nucl Med Mol Imaging* 2021; **48**:4495–4507.
- 22 Hoberück S, Löck S, Borkowetz A, Sommer U, Winzer R, Zöphel K, et al. Intraindividual comparison of [<sup>68</sup>Ga]-Ga-PSMA-11 and [<sup>18</sup>F]-F-PSMA-1007 in prostate cancer patients: a retrospective single-center analysis. *EJNMMI Res* 2021; **11**:109.
- 23 Pattison DA, Debowski M, Gulhane B, Arnfield EG, Pelecanos AM, Garcia PL, et al. Prospective intra-individual blinded comparison of [<sup>18</sup>F]PSMA-1007 and [<sup>68</sup>Ga]Ga-PSMA-11 PET/CT imaging in patients with confirmed prostate cancer. *Eur J Nucl Med Mol Imaging* 2022; **49**:763–776.
- 24 Ninatti G, Pini C, Gelardi F, Ghezzi S, Mapelli P, Picchio M, et al. The potential role of osteoporosis in unspecific [<sup>18</sup>F]PSMA-1007 bone uptake. *Eur J Nucl Med Mol Imaging* 2023; **51**:304–311.
- 25 Luo L, Wang Z, Wang X, Gao J, Zheng A, Duan X. Fluorine-18 prostate-specific membrane antigen-1007-avid indeterminate bone lesions in prostate cancer: clinical and PET/CT features to predict outcomes and prognosis. *Clin Radiol* 2024; **79**:346–353.
- 26 Chiu LW, Lawhn-Heath C, Behr SC, Juarez R, Perez PM, Lobach I, et al. Factors predicting metastatic disease in <sup>68</sup>Ga-PSMA-11 PET-positive osseous lesions in prostate cancer. *J Nucl Med* 2020; **61**:1779–1785.
- 27 Phelps TE, Harmon SA, Mena E, Lindenberg L, Shih JH, Citrin DE, et al. Predicting outcomes of indeterminate bone lesions on <sup>18</sup>F-DCFPyL PSMA PET/CT scans in the setting of high-risk primary or recurrent prostate cancer. *J Nucl Med* 2023; **64**:395–401.
- 28 Rizzo A, Morbelli S, Albano D, Fornarini G, Cioffi M, Laudicella R, et al. The Homunculus of unspecific bone uptakes associated with PSMA-targeted tracers: a systematic review-based definition. *Eur J Nucl Med Mol Imaging* 2024; **51**:3753–3764.
- 29 Kroenke M, Mirzoyan L, Horn T, Peeken JC, Wurzer A, Wester HJ, et al. Matched-pair comparison of <sup>68</sup>Ga-PSMA-11 and <sup>18</sup>F-rhPSMA-7 PET/CT in patients with primary and biochemical recurrence of prostate cancer: frequency of non-tumor-related uptake and tumor positivity. *J Nucl Med* 2021; **62**:1082–1088.
- 30 Chen MY, Franklin A, Yaxley J, Gianduzzo T, McBean R, Wong D, et al. Solitary rib lesions showing prostate-specific membrane antigen (PSMA) uptake in pre-treatment staging <sup>68</sup>Ga-PSMA-11 positron emission tomography scans for men with prostate cancer: benign or malignant? *BJU Int* 2020; **126**:396–401.
- 31 Seifert R, Emmett L, Rowe SP, Herrmann K, Hadaschik B, Calais J, et al. Second version of the prostate cancer molecular imaging standardized evaluation framework including response evaluation for clinical trials (PROMISE V2). *Eur Urol* 2023; **83**:405–412.
- 32 Zacho HD, Ravn S, Afshar-Oromieh A, Fledelius J, Ejlersen JA, Petersen LJ. Added value of <sup>68</sup>Ga-PSMA PET/CT for the detection of bone metastases in patients with newly diagnosed prostate cancer and a previous <sup>99m</sup>Tc bone scintigraphy. *EJNMMI Res* 2020; **10**:31.
- 33 Jakanani GC, Saifuddin A. Percutaneous image-guided needle biopsy of rib lesions: a retrospective study of diagnostic outcome in 51 cases. *Skeletal Radiol* 2013; **42**:85–90.
- 34 Miszczyk M, Rajwa P, Yanagisawa T, Nowicka Z, Shim SR, Laukhtina E, et al. The efficacy and safety of metastasis-directed therapy in patients with prostate cancer: a systematic review and meta-analysis of prospective studies. *Eur Urol* 2024; **85**:125–138.
- 35 De Coster L, Sciort R, Everaerts W, Gheysens O, Verscuren R, Deroose CM, et al. Fibrous dysplasia mimicking bone metastasis on (<sup>68</sup>Ga)-PSMA PET/MRI. *Eur J Nucl Med Mol Imaging* 2017; **44**:1607–1608.